iJETRM
International Journal of Engineering Technology Research & Management
(IJETRM)
https://ijetrm.com/

SEPIC-CUK BASED ELECTRIC VEHICLE CHARGING SYSTEM WITH BATTERY STORAGE FOR ENHANCED EFFICIENCY

N. Deena Nepolian
ECE Department, Assistant Professor,
Annai Vailankanni College of Engineering, Kanyakumari, India

Jeba P S
ECE Department, Assistant Professor,
Mar Ephrem College of Engineering and Technology, Elavuvilai Kanyakumari, India

Swapna C S
ECE Department, Assistant Professor,
Annai Vailankanni College of Engineering, Kanyakumari, India

C.R. Manoj
EEE Department, Assistant Professor,
Bethlahem Institute of Engineering, Kanyakumari, India

ABSTRACT
Electric Vehicles (Evs) have enlarged significant popularity owing to their environmental benefits and the enhancing demand for sustainable transportation. Integrating renewable energy sources such as photovoltaic systems for EV charging improves the sustainability and cost effectiveness of overall system. For improving the overall performance and reliability of EV charging systems, an effectual continuous charging of EV batteries is crucial. Therefore, this paper introduces a novel topology to optimal EV charging by utilizing an integrated SEPIC-Cuk converter with energy management system. The integrated SEPIC-Cuk converter is developed for enhancing the voltage obtained from PV, which offers high voltage gain with reduced component count. Moreover, to control the converter operation, the Chaotic dragon fly optimization (CDO) based PI controller is used, it provide the stable output voltage with better convergence speed and robustness. The battery system gets charged by the PV system for EV charging and the bidirectional converter is employed for both charging and discharging purpose as per the battery needs. Additionally, the excess energy obtained from the PV system after supplying enough power to the battery is deliver to the grid system through single VSI. During unavailable power from PV, the grid flows in bidirectional for charging the battery, thus continuous power supply is fed to battery system. To validate the effectiveness of the developed system it is executed in MATLAB/Simulink and the comparative analysis is made over with the traditional topologies for showing the prominence of the proposed work. The outcomes illustrates that the proposed converter approach has high voltage gain ratio of 1:10, high efficiency of 97.42% as well as minimized THD value of 2.42%. Thereby, this research contributes to the ongoing efforts in developing advanced charging solutions with energy management system.

Keyword-
EV, RES, PV, SEPIC-Cuk Converter, CDOA, MATLAB.

I. INTRODUCTION

In recent era, sustainable energy-based transportation solutions have drawn more attention from the government, automakers, and consumers in the form of zero-emission vehicles like EVs and electric automobiles, etc. The electrification of transportation is increasing daily [1] in order to reduce reliance conventional fuels and to lessen the accompanying climate implications. The electric vehicles (EVs) that operate by battery packs offer extra environmental benefits. To help alleviate major worries about rising pollution and its negative effects, the transition from traditional electric energy generation, that uses fossil fuels, to one focused on green energy must prioritize mobility. However, there's additional technological considerations to be made if EVs are going to be linked to the electric power grid for charging [2]. Initially the energy composition

iJETRM
International Journal of Engineering Technology Research & Management
(IJETRM)
https://ijetrm.com/

of any local electric power system affects the indirect emissions of EVs. However, the pollution benefit for EVs is not clear if coal-fired power plants account for a large portion of the electrical system's power output. To satisfy charging need, successfully boost EV emission reduction, and lessen reliance on the power grid, RES must be directly integrated with electric vehicle (EV) charging facilities [3]. The consumption of electricity to support human life's necessities is crucial to a nation's economic development. Solar cells are energy generators that can transform solar energy into electrical current. The usage of solar cells can lead to issues because the amount of electricity generated depends upon environmental factors like temperature and light intensity, keeping the system's power output unstable [4]. Consequently, a battery is required that holds the energy generated throughout the process of irradiation to ensure the entire system has the energy stored in the battery in case the solar cell fails to absorb sunlight. In recent years, sustainable energy-based transportation solutions have drawn more attention from the government, automakers, and consumers in the form of zero-emission vehicles like EVs and electric automobiles, etc. The primary source of power for EVs is a lead acid battery, which requires an effective charger to continually power the EV and other accessories.Battery lifespan is impacted by ripple current [5, 6]. DC-DC converters are crucial to produce higher voltage obtained from the PV system, there are several DC-DC converters used for application using renewable energy which remain a more attractive and feasible solution to combine with RES , despite the fact that both groups have their own benefits and drawbacks [7].

For PV uses, Buck-Boost, SEPIC, Zeta, and Cuk are the most often used non-isolated converters [8]. These converters' Boost and Buck topologies provide low-order circuits, outstanding effectiveness, and flexibility. However, its rigidity with regard to output voltage can limit their use. Boost converters and Buck converters are able to increase or decrease voltage. Consequently, both Boost and Buck converters are inappropriate to charge battery uninterruptedly with MPPT operation, like in the case of PV system battery charging. MPP tracking is not feasible in a Boost converter if the battery voltage is less than the PV panel's extreme power voltage; on the contrary present, MPP tracking is not feasible in a Buck converter if the battery voltage is greater [9-11]. It is possible to perform MPP tracking using Buck-Boost, SEPIC, Zeta, and Cuk topologies independent of modifications to the environment and the linked load because it produce an output voltage that is greater or lower compared to the PV generator. Because of its adaptable output gain, SEPIC functions as a buck-boost DC-DC converter, changing its output voltage in accordance with its duty cycle [12]. The Cuk converter eliminates any such restrictions and offers advantages like low input and output current ripples, which makes it a natural choice for PQ enhancement in EV chargers. The high current strain between the parts, however, prevents the aforementioned methods from being used in the majority of high-power ac-dc converter systems [13,14]. An example of a non-isolated converter is the SEPIC-Cuk converter, which has two operating modes: boost mode and buck mode [15]. In this study, a converter system that works to charge batteries from solar panels is created utilizing a SEPIC-Cuk type converter.

The PI controller is popular for being sensitive to changes in parameters, weather, and other variables. In order to manage variables like unpredictable weather for the PV system, a more effective controller must be used [16, 17]. Particle Swarm Optimization (PSO), Perturb and Observe (P&O), Genetic Algorithm (GA), Crow Search (SC), and Firefly Algorithm (FA), among others are some of the optimization approaches that have been created over time. The efficiency, cost, monitoring speed, monitoring accuracy, and hardware needs of all of these systems differ in a number of ways. They perform admirably in the majority of situations, but they are challenging to execute on a cheap digital controller [18-23]. This study uses the chaotic dragon fly optimization technique, a well-known category of meta-heuristics that draws its inspiration from dragonflies. The conventional previous work has resulted that the PV generator's insufficient treatment as an input for power electronics conversion devices, which could be a factor in the dependability problems with PV energy systems that have been identified. Among the most basic approaches to synchronize a power converter to the electrical network is to divide the current reference signal by the grid voltage. In order to maintain unity power factor, the grid-tied converter is typically necessary, and it is regulated to avoid islanding in the case of grid failure [24, 25].

In this paper, a SEPIC-Cuk Converter is developed along with CDO algorithm based PI controller to improve energy flow of a grid integrated PV system. The converter efficiently matches the PV panel voltage with the grid voltage, permitting seamless power injection into the grid. The CDO algorithm-based PI controller dynamically tunes the converter's control parameters to regulate the output voltage. There are five sections in this work. The proposed technique is addressed in section II after the introduction. The CDO algorithm, design, and modelling are covered in section III. Section IV presents the findings and discussions.

International Journal of Engineering Technology Research & Management
(IJETRM)
https://ijetrm.com/

II. PROPOSED SYSTEM

In the pursuit of efficient and sustainable energy solutions, grid-integrated PV systems play a essential role by harnessing solar energy and injecting it into the power grid. To optimize energy flow and maximize power extraction from PV panels, the concept of employing the SEPIC-Cuk Converter along with a CDO algorithm-based PI controller is used. The designed system's overall layout as represented in Figure 1. The system is comprised of PV modules, a DC-DC converter, a battery and a grid.

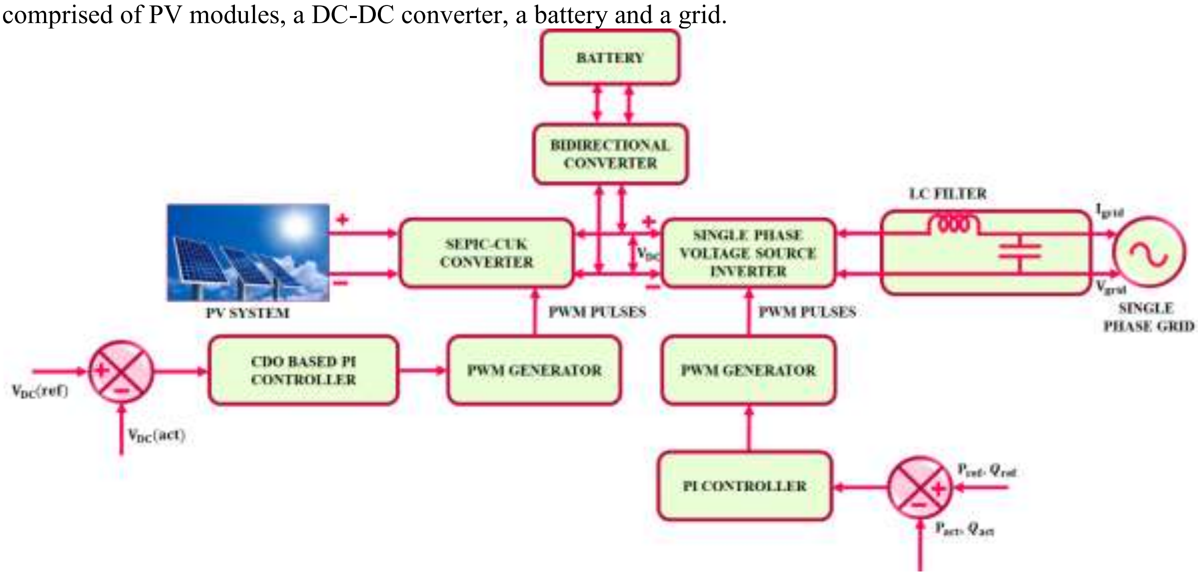

Figure 1 Proposed System block diagram

In this research, a battery is charged using a PV module and the Interleaved SEPIC-Cuk converter is used for boosting the voltage from PV to satisfy required level of battery and grid system. The converter is controlled with the aid of PI that results in a slower output response and its parameter needs to tune for better performance. Therefore, the chaotic dragonfly optimized control approach is utilized to provide a faster response from an output and control the output voltage of converter. The enhanced power is deliver to the PWM generator for producing needed pulses for the better switching operation of the converter. Additionally, during excess power generation form PV system after supplying enough power to battery for EV charging, the grid gets energized through the single phase VSI that provide power by converting DC-AC supply and regulated by the PI controller. During insufficient power from PV system the grid provide alternate power to battery and the bidirectional converter is utilized for regulating the battery bank for charging and discharging process, while sustaining the battery's SOC within safe limits. Finally, the continuous power supply is given to battery system for EV charging without any interruptions.

MODELLING OF THE PROPOSED SYSTEM

A. SOLAR PV MODEL

A solar cell is a device, which utilizes the PV to transform solar energy into electrical energy. When two electrodes attached to a solid or liquid system make interaction with one another, a phenomena known as the solar energy effect occurs. This phenomenon causes an electric voltage to arise. Due to the energy of photons of sunshine that is effectively liberated and allowed to move in a type N and P semiconductor connection, electric current is created. This solar cell includes an optimistic foot and a negative foot that are linked to a network or equipment that needs a power supply, similar to a photodiode.

iJETRM
International Journal of Engineering Technology Research & Management
(IJETRM)
https://ijetrm.com/

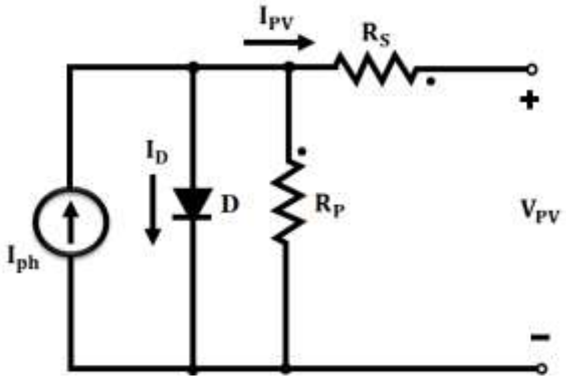

Figure 2. PV panel equivalent circuit

PV modelling equation using 1 diode,

$$I_{PV} = I_{PVn} - (I_0 \left(\frac{V_0}{e^{aV_\tau}} - 1\right) - \frac{V_{PV} + I_{PV} R_S}{R_P} \tag{1}$$

Where, I_{PV} represents the PV output current and R_S, R_P denotes the series and parallel resistors respectively. I_0 is the Reverse Saturation Current and a is the diode ideality factor and V_τ represents the thermal voltage.Under varied solar cell working situations, the converter is given to control the steady output voltage, and in this case, the SEPIC-Cuk converter is used to deliver greater voltage gain from the PV.

B. SEPIC - CUK CONVERTER

Photovoltaic DC-DC converters are a vital part of PV energy conversion. In various solar cell usage scenarios, the DC-DC SEPIC-Cuk converter is available to adjust the constant output. This study makes use of Integrated Sepic-Cuk Converter, a non-isolated converter kind that may be used in either boost mode or buck mode. Since the period of operation of the SEPIC and Cuk converters is identical, the output voltage is also comparable. According to the duty cycle, this converter can performs as a boost or buck converter.

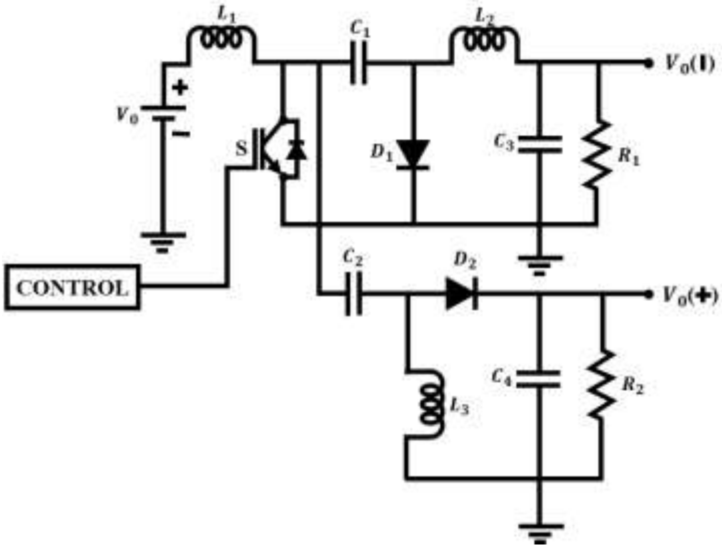

Figure 3.Circuit diagram of SEPIC-Cuk Converter

iJETRM
International Journal of Engineering Technology Research & Management
(IJETRM)
https://ijetrm.com/

The converter performs boost operation if its duty cycle level exceeds, the voltage responsiveness of the SEPIC converter changes to positive, and the voltage response of the Cuk changes to negative. The output voltage level vary according to the orientations of the SEPIC and Cuk converters when the duty cycle is less than 50%, acting as a buck converter. As demonstrated in Figure 3, the SEPIC and Cuk converters' ability to integrate the two components allows for the creation of bipolar type converters. Both the SEPIC side and the Cuk side of the converters operated by a single switch. Since the switch has been linked to the ground, there is no requirement for synchronizing additional switches. There are two operational modes for the bipolar SEPIC-Cuk converter circuit, including

Mode 1

When switch S is activated, L_1 *and* L_2 retain the energy generated by the input voltage. Because of the depletion of capacitors C_1 *and* C_2, the L_3 *and* L_4 inductors additionally serve as devices for storing energy. The drifting diode is inactive or open throughout this time. The output capacitor delivers the energy going to load.

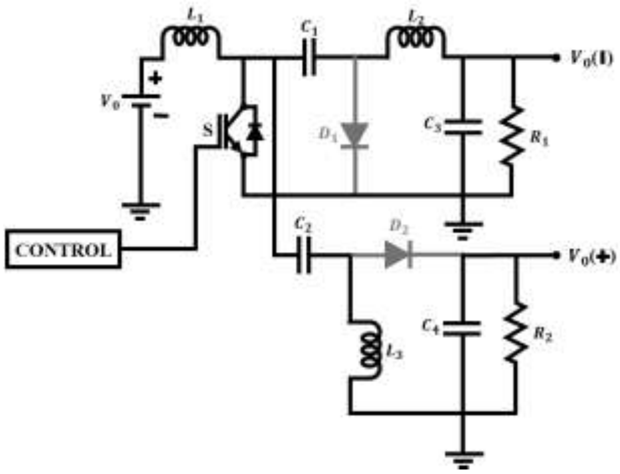

Figure 4. Circuit operation of mode1

Mode 2

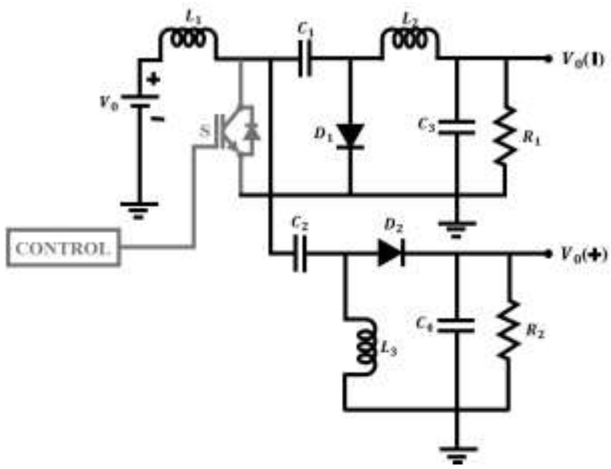

Figure 5. Circuit operation of mode 2

International Journal of Engineering Technology Research & Management
(IJETRM)
https://ijetrm.com/

The inductor charges the capacitors C_1 *and* C_2 by way of freewheeling diodes D_1 *and* D_2 and powers the load while the S switch is off. The SEPIC-Cuk converter's output voltage is as a result,

$$V_O = -V_S(\frac{D}{1-D}) \tag{2}$$

Applying the subsequent the formula, find the inductor and capacitor values for the SEPIC,

$$L_1 = L_2 = \frac{V_S.D}{\Delta IL.f} \tag{3}$$

$$C_1 = C_2 = \frac{V_{out}.D}{R.\Delta V_O.f} \tag{4}$$

Applying the subsequent the formula, get the current value of the Cuk Inductor and capacitor is,

$$L_1 = \frac{V_S.D}{\Delta IL_1.f} \tag{5}$$

$$L_2 = \frac{V_S.D}{\Delta IL_2.f} \tag{6}$$

$$C_1 = \frac{V_{out}.D}{R.\Delta VC_1.f} \tag{7}$$

$$C_2 = \frac{1-D}{R.L_2.{}^{\Delta V_o}/_{V_{out}}f^2} \tag{8}$$

where, V_{Out} is the output voltage , D represents duty cycle and ΔIL is ripple current across inductor.

iJETRM
International Journal of Engineering Technology Research & Management
(IJETRM)
https://ijetrm.com/

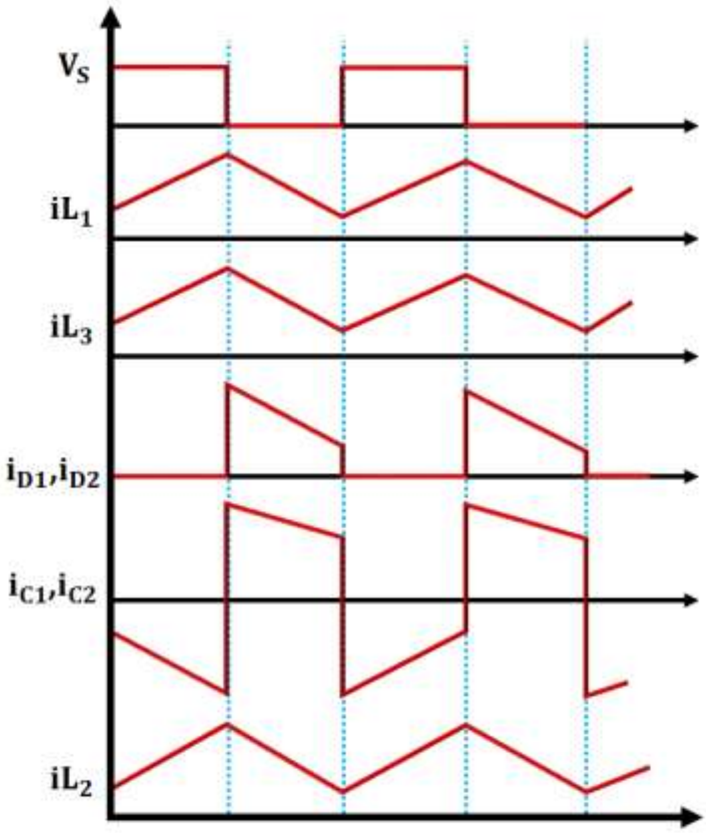

Figure 6. Modes of SEPIC-Cuk Converter

The converter integrates SEPIC and a Cuk, which have the same voltage converting ratio, polarity of opposite, and a mixture of active and passive components. There is a single switch that control both configurations and the control circuit is not complicated since the control terminal is grounded. These topologies are helpful for creating bipolar dc link type converters because they combine two converters that may provide an output of the same magnitude but with a reverse polarity.

C. CHAOTIC DRAGONFLY ALGORITHM BASED PI CONTROLLER

The Chaotic Dragonfly Optimized PI Controller for maintaining constant DC link voltage is a specialized control system designed for applications involving DC-DC converters or similar power electronic systems. In such systems, it is essential to maintain the DC link voltage to a constant value to ensure stable and reliable operation. The PI controller is a widely used control technique in power electronics to achieve regulation and control of output variables, such as voltage or current. In this case, optimized PI controller is utilized to maintain the DC link voltage and keep it at a desired setpoint.

The chaotic dragonfly optimization algorithm (CDOA) is modelled after the hunting and movement of dragonfly swarms in nature. The sine-cosine and chaos-based CDOA method is an enhancement on the DA technique. The DA method and CDOA technique are both put to the test using eight test parameters. The revised CDOA approach has better resolution precision than the DA algorithm, and it is more stable than the initial DA algorithm.

iJETRM
International Journal of Engineering Technology Research & Management
(IJETRM)
https://ijetrm.com/

Figure 7. CDOA Flowchart

Equation (9) represents the symbolic illustration of the dragonfly method.

$$\begin{cases} \Delta X_{t+1} = (sS_i + aA_i + cC_i + fF_i + eE_i) + w\Delta X_i \\ X_{t+1} = X_t + \Delta X_{t+1} \end{cases} \tag{9}$$

Assuming there aren't any nearby agents, formula (10) is used to modify the location of the agents. X_t indicates the location of the agents at the t-th iteration; X_{t+1} reflects the step size of the modification.

$$X_{t+1} = X_t + Levy(d)X_t \tag{10}$$

where d is the location vector's magnitude. Equation (11) is used to denote the Levy function.

$$Levy(x) = \frac{0.01 r_1 \sigma}{|r_2|^{\frac{1}{\beta}}} \tag{11}$$

Where is a variable set to 3/2 and r_1 and r_2 are the random numbers between [0, 1], is determined using formula (12).

IJETRM
International Journal of Engineering Technology Research & Management
(IJETRM)
https://ijetrm.com/

$$\sigma = \left(\frac{\tau(1+\beta)\sin\left(\frac{\pi\beta}{2}\right)}{\tau\left(\frac{1+\beta}{2}\right)\beta\, 2^{\left(\frac{\beta-1}{2}\right)}}\right)^{\frac{1}{\beta}} \tag{12}$$

Where $\tau(x) = (x-1)!$ (13)

Table 1: Parameters of CDA

Parameter Details (CDA)	Value
β	1.5
d	31
M	50
Lower bound	1
Upper bound	31
MaxIteration	50

Algorithm of the Chaotic Dragonfly Optimization Algorithm is given by,
Step 1: Set the dragonfly population. X_i(i=1, 2,…, n)

Set the step vectors ΔX_i(i=1, 2,…, n)

While (iteration $\leq$ MaxIteration)

Step 2: To calculate the prime parameters of DA
Calculate the overall dragonflies' objective values.
Modify the enemy and food sources
Update neighbouring radius
Number of neighbour has been evaluated
Step 3: To update location vector
Assuming a dragonfly has a minimum of one neighbour,
Update step vector and location vector
End if
Check and adjust the new position using the variable boundary information.
End while

By utilizing the chaos-driven optimization approach, the control system efficiently respond to variations and uncertainties, leading to improved performance and robust regulation of the DC link voltage in real-world applications. The proposed CDOA algorithm has the benefit of accurate loss computation and exact estimate. Subsequently, the rate of convergence improves as exploitation potential increases.

D. BIDIRECTIONAL CONVERTER

The bidirectional battery converter is a vital component in EV charging system, as it allows energy to flow bidirectionallity, enabling both charging and discharging operations. By utilizing this converter topology, which operate in both Buck and Boost modes with the capable of stepping up and stepping down the voltage as required to maintain the compatibility over the battery voltage as illustrated in Figure 8.

iJETRM
International Journal of Engineering Technology Research & Management
(IJETRM)
https://ijetrm.com/

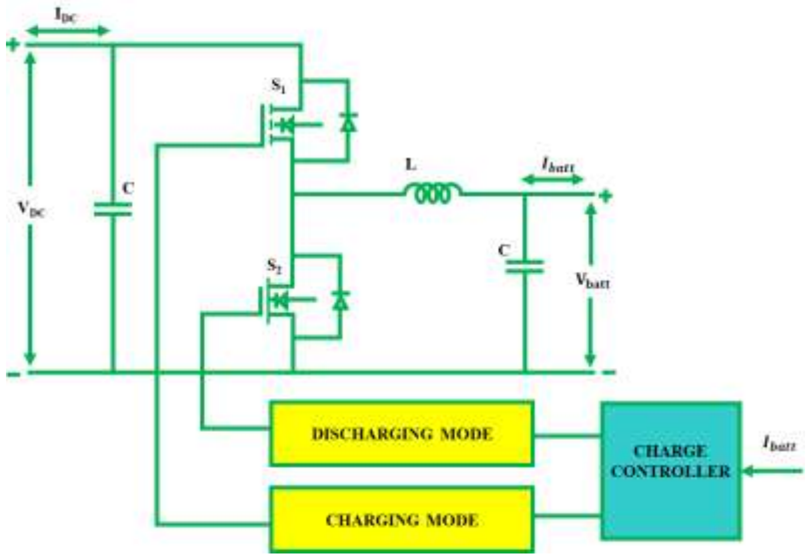

Figure 8 Structure of Bidirectional converter

Buck Mode: In this mode, the converter steps down the battery voltage to match the charging system voltage. As specified in Figure, during S1 is in ON condition the input current enhances and moves through S1 and L and the battery gets charging over the grid. Additionally, during S_1 is in OFF state the inductor current minimizes and inductor L generates the power required to charge battery system.

Boost Mode: In boost mode, this converter steps up the voltage to match the charging system voltage, at this mode, the output voltage is greater than the input voltage during the energy discharged from the load. During switch is ON condition, input current enhances over S_1 and the inductor current reduced until the S2 is in OFF state.

E. SINGLE PHASE VSI

The single phase VSI is utilized for converting DC supply to AC for distributing power to the grid system. A two-arm single phase full bridge inverter with two semiconductor switches on each arm and opposite freewheeling diodes for each switch for draining the opposite current are used . In the context of RL load devices, these diodes often enable reverse load current to pass over it and also offer a different route to inductive current, which continues to run in this manner under the Turn OFF scenario as represented in Figure 8.

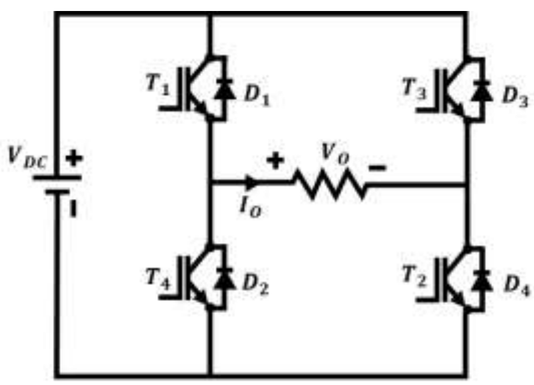

Figure 9. Circuit diagram of single phase full-bridge VSI

iJETRM
International Journal of Engineering Technology Research & Management
(IJETRM)
https://ijetrm.com/

The switches in Figure 9 are T_1, T_2, T_3 and T_4 and the didoes are opposite freewheeling D_1, D_2 and D_3 .On every connection, the switches work alternately in order to prevent them from being ON and OFF in the same mode at the same time. In order to prevent short circuiting, both switches are typically turned off for a very brief period of time known as blanking time. The switches must be operated in pairsT_1 and T_2 or T_3 and T_4 to provide the appropriate output. Using the Pulse Width Modulation technology to precisely provide switching pulses to the MOSFET has improved power conversion from DC to AC with minimal losses and low THD in output.

III. RESULTS AND DISCUSSION

The electricity generated from solar cells is enhanced using a SEPIC-Cuk converter and then converted to AC power employing a single phase VSI system utilizing MATLAB program. Table 2 displays the parameter requirements for the PV system and the SEPIC-Cuk converter.

Table 2: Parameter Specifications

Parameters	Rating
PV system	
Peak power	10 KW
Capacity	$5W$
Number of panels	20
SEPIC-Cuk converter	
L_1, L_2	$1.2mH$
C_1	$4.7\mu F$
C_2	$22\mu F$

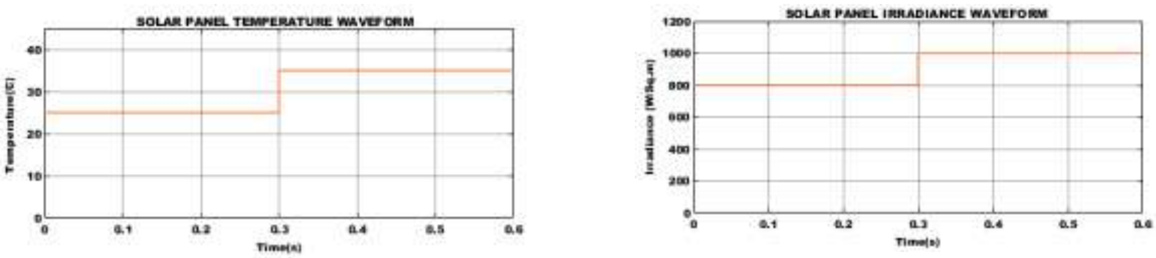

(a) (b)

Figure 10. Solar Parameter Waveforms (a) Temperature and (b) Irradiation

Figure 10 depicts the characteristics of the solar PV system for temperature and radiation. It is seen that the temperature starts off at 25°C and then rises to reach an average temperature of 35°C. Similarly, the starting irradiation amount of 800W/sq m is maintained; however, after 0.3s due to an increase in temperature, the panel achieves an irradiation level of 1000W/sq m, giving sufficient supply to the converter input.

iJETRM
International Journal of Engineering Technology Research & Management
(IJETRM)
https://ijetrm.com/

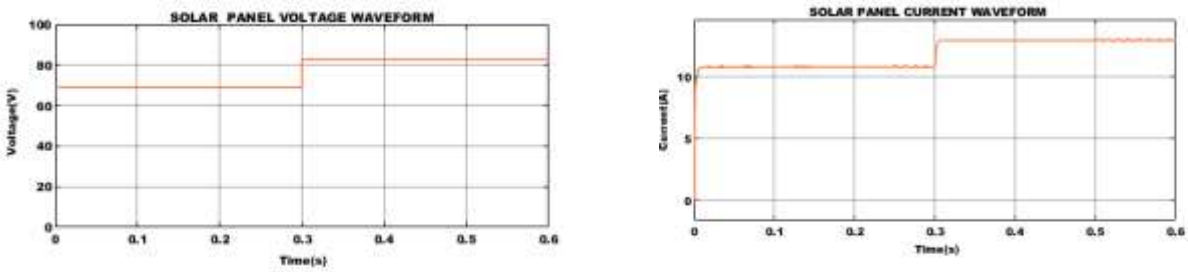

(a) (b)

Figure 11. Solar Parameter Waveforms (a) Voltage and (b) Current

Figure 11 shows the waveform of the electrical voltage and current reaching the SEPIC-Cuk converter from the solar panel. An initial input voltage of 70V is reached and maintained for 0.3 seconds; afterwards, because of a rise in the PV parameter, the voltage increases to 82V and continues to be maintained. According to this, after 0.3 seconds of peak growth in PV current during the first phase, a steady current level of 14A is reached.

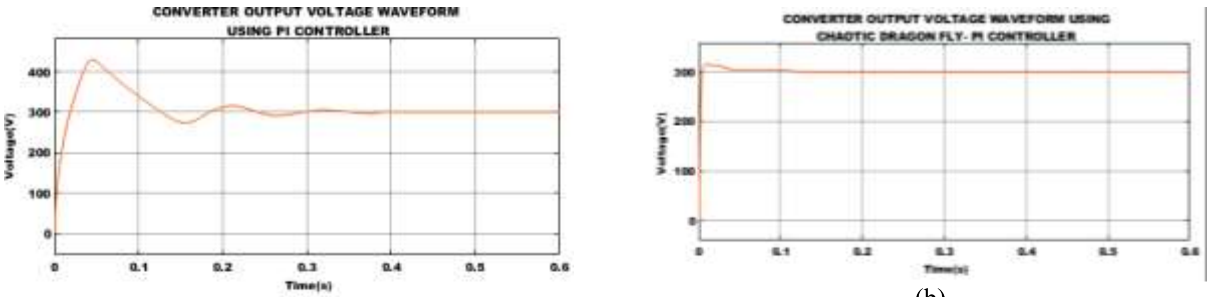

(a) (b)

Figure 12. Output Voltage of Proposed Converter by adopting (a) PI, (b) CDOA-PI.

Figure 12 shows how the SEPIC-Cuk converter output voltage was accomplished by using CDOA-PI and PI controllers to regulate the DC link supply. It is clear from Figure 12(a) that tuning is required because using a PI controller does not produce a steady voltage result of 300V. In Figure 12(b), the CDOA-tuned PI controller produces output that is stable. Therefore, a CDOA-PI controller is suggested in order to attain stable DC voltage as quickly as possible, producing stabilized DC voltage of 300V.

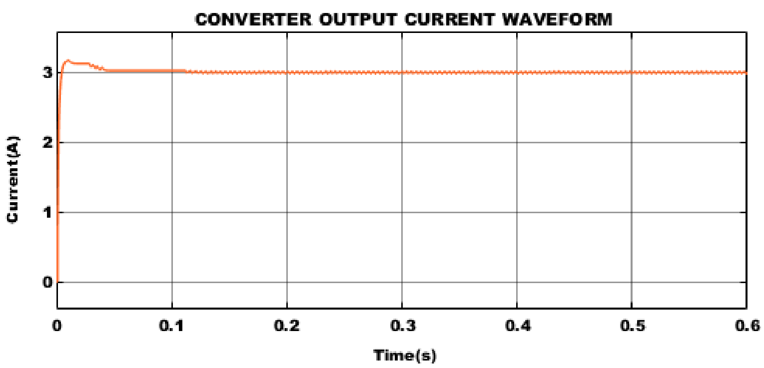

Figure 13. Converter Output Current

iJETRM
International Journal of Engineering Technology Research & Management
(IJETRM)
https://ijetrm.com/

Figure 13 shows the appropriate output current from the SEPIC-Cuk converter. The current is seen to fluctuate in the early stages before stabilizing after 0.025s and maintaining a constant current value of 3A.

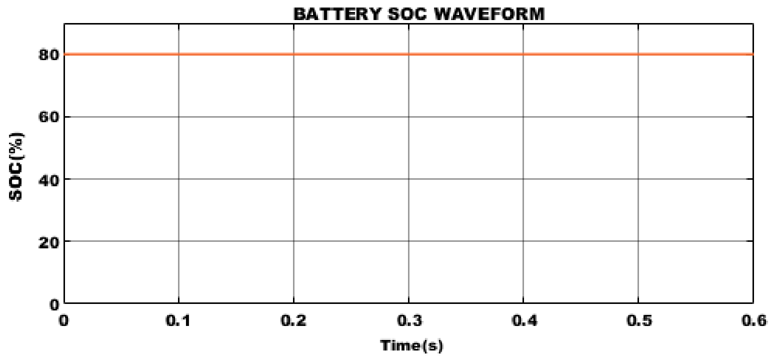

Figure 14. SOC of the battery

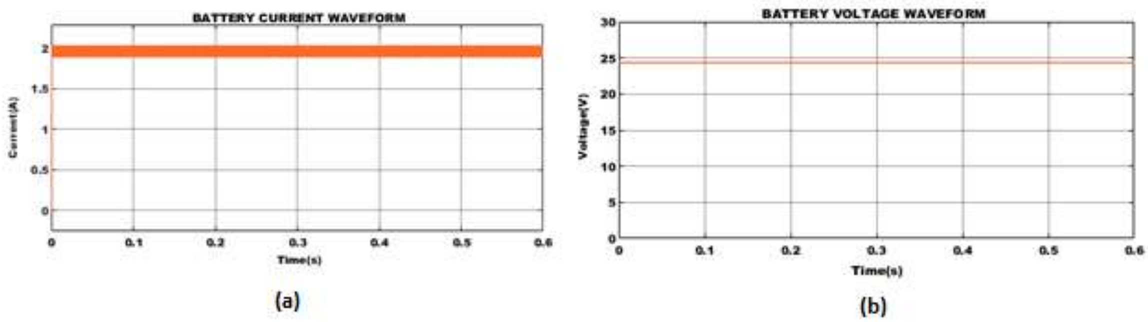

Figure 15.Battery (a) Current (b) Voltage

With a continuous current of 2A and a battery voltage of 24 V, the battery cell was running. The battery's SOC then achieves 80%.

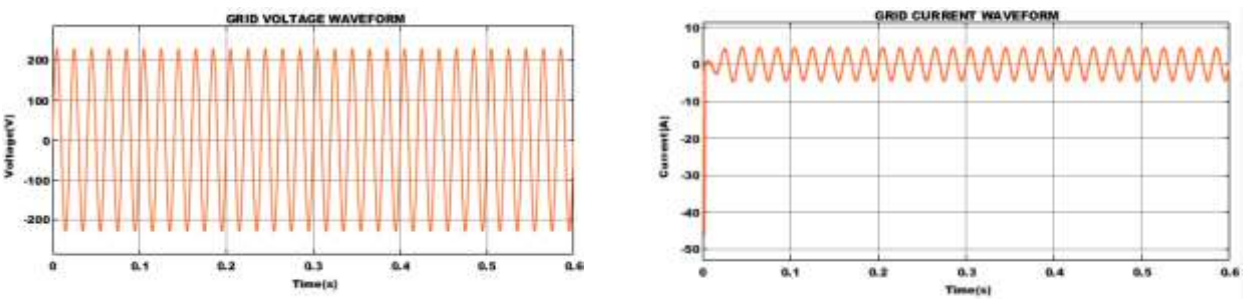

(a) (b)

Figure 16. 1Φ Grid (a) Voltage and (b) Current

iJETRM
International Journal of Engineering Technology Research & Management
(IJETRM)
https://ijetrm.com/

Figures 16(a) and (b) show the voltage and current waveform of a single-phase grid, which represents the varying patterns of electrical energy. These waveforms provide a constant and steady flow of electricity with effective power transmission, efficient functioning of electrical devices, and maintenance of a stable network because of regulated voltage and current.

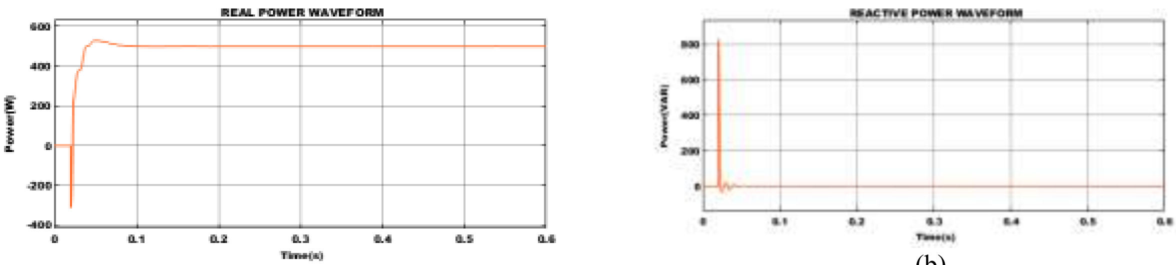

(a) (b)

Figure 17. (a) Real and (b) Reactive Power Waveform

Figure 17 depicts the waveforms illustrative of actual power and reactive power. It is observed that after experiencing a few slight variations at first, the true power stabilizes about 500W. Reactive power, on the contrary, is the first oscillating power that results from the existence of inductive or capacitive devices, generating voltage and current phase variations, and it eventually diminishes. Moreover, the power factor for the developed work is maintained unity as illustrtaed in Figure 18.

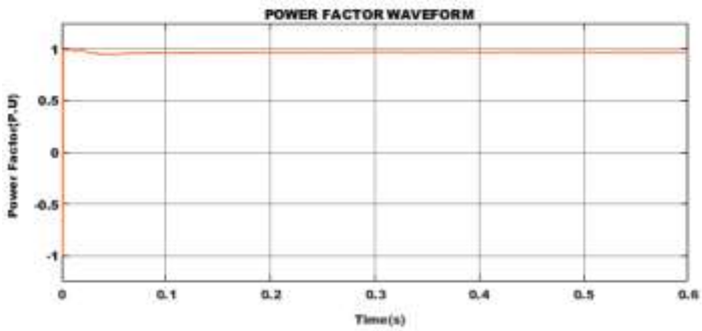

Figure 18. Power factor waveform

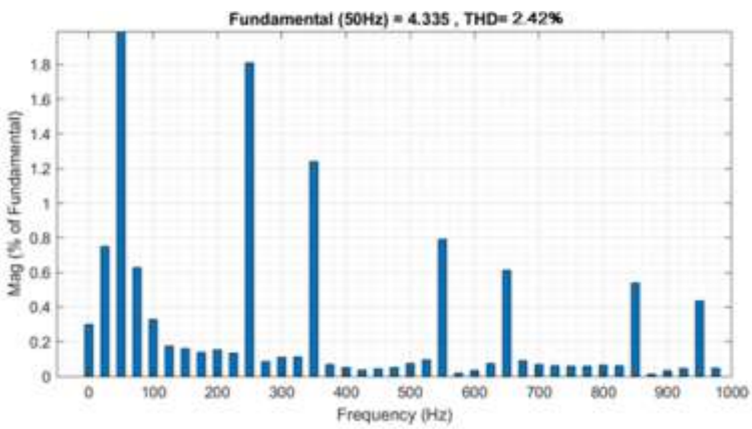

Figure 19. THD Value

iJETRM
International Journal of Engineering Technology Research & Management
(IJETRM)
https://ijetrm.com/

The examination of the THD performance of the grid-connected PV system as illustrated in above Figure 19, which indicates 2.42%. This indicates that the PV system is generating clean and high-quality power, with minimal levels of harmonic distortion introduced into the grid. It also ensures better compatibility with the grid, reducing the risk of grid instability.

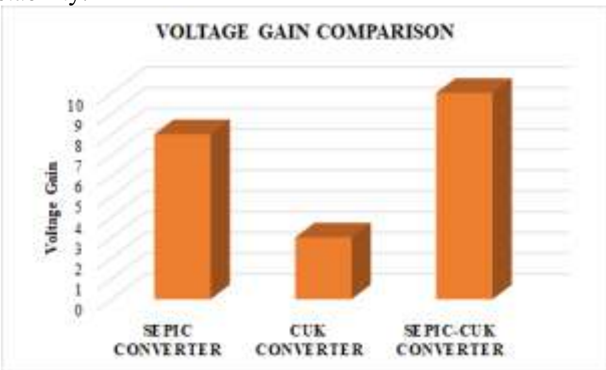

Figure 20. Comparison of Voltage gain

The developed SEPIC-Cuk converter architecture is compared to conventional converters in an analysis based on voltage gain, as shown in Figure 20. According to investigation, the proposed converter obtained increased voltage gain of 1:10.

Table 3: Comparison of Converter Performance

Converters	Voltage gain	Efficiency (%)
SEPIC	$\frac{D}{(1-D)}$=8	94.5 % [26]
Cuk	$\frac{1}{1-D}=3$	92 % [27]
SEPIC-Cuk	$(\frac{1-D}{1+D})$=10	97.42%

Table 3 the results of comparing the proposed converter performance with that of standard SEPIC and Cuk converters. It has been demonstrated that the proposed Integrated SEPIC-Cuk converter topology performs better than SEPIC and Cuk converter topology in regards to 97.42% efficiency and 1:10 voltage gain. This indicates that the PV system efficiently step up the low DC voltage produced by the solar panels to a maximum voltage level suitable for grid integration.

Table 4: Controller Performance Analysis

Performance Measures	PI	CDOA-PI
Peak Time (T_p) in sec	0.05	0.02
Rise Time (T_r) in sec	0.02	0.01
Settling Time (T_s) in sec	0.42	0.12

The results of optimizing the PI controller variables to produce better converter functioning are shown in Table 4 along with the associated outcomes. As shown in Figure 11, the suggested CDOA-PI controller achieves

iJETRM
International Journal of Engineering Technology Research & Management
(IJETRM)
https://ijetrm.com/

a stabilized voltage of 300V earlier than the standard PI controller at a time of 0.02s. Thus the proposed system quickly and accurately responds to changes in operating conditions, such as varying solar irradiance, load demands, and grid conditions.

IV. CONCLUSION

Due to rising population and energy demand, a larger range of people are using Evs, to charge EV the RES based PV is employed, which helps with EV charging today and is becoming more significant. Furthermore, the primary task of an EV system is charging the batteries, and traditional methods of charging have a variety of drawbacks, including poor energy management, interrupted power supplies, and short battery life. Therefore, a novel EV charging station is presented in the developed work and it makes use of an improved DC-DC Bi-directional SEPIC-Cuk converter which provides voltage gain ratio of 1:10. In this setup, the EV battery receives power directly from the PV panel, and any extra power generated by the PV is fed into the grid. The developed converter operates in boost mode and helps to increase PV output; the consequent DC-link voltage is controlled and kept steady utilizing the Chaotic Dragon fly technique with an efficiency of 97.42%. The grid also receives the DC link voltage via $1\emptyset$ VSI and grid synchronization is attained by using a PI controller which

provide THD value of 2.42%.

REFERENCES

1) S. -K. Lim, H. -S. Lee, H. -R. Cha and S. -J. Park, "Multi-Level DC/DC Converter for E-Mobility Charging Stations," in IEEE Access, vol. 8, pp. 48774-48783, 2020.
2) Jiang, Wei, and Yongqi Zhen. "A real-time EV charging scheduling for parking lots with PV system and energy store system." *IEEE Access* ,Vol.7 , pp: 86184-86193,2019.
3) B. Zeng, H. Dong, F. Xu and M. Zeng, "Bilevel Programming Approach for Optimal Planning Design of EV Charging Station," in IEEE Transactions on Industry Applications, vol. 56, no. 3, pp. 2314-2323, May-June 2020.
4) Guisández Hernández and S. P. Santos, "Modelling and Experimental Validation of Aging Factors of Photovoltaic Solar Cells," in IEEE Latin America Transactions, vol. 19, no. 8, pp. 1270-1277, Aug. 2021.
5) Q. Yan, B. Zhang and M. Kezunovic, "Optimized Operational Cost Reduction for an EV Charging Station Integrated With Battery Energy Storage and PV Generation," in IEEE Transactions on Smart Grid, vol. 10, no. 2, pp. 2096-2106, March 2019.
6) U. B. Irshad, M. S. H. Nizami, S. Rafique, M. J. Hossain and S. C. Mukhopadhyay, "A Battery Energy Storage Sizing Method for Parking Lot Equipped With EV Chargers," in IEEE Systems Journal, vol. 15, no. 3, pp. 4459-4469, Sept. 2021.
7) V. Karthikeyan, S. Kumaravel and G. Gurukumar, "High Step-Up Gain DC–DC Converter With Switched Capacitor and Regenerative Boost Configuration for Solar PV Applications," in IEEE Transactions on Circuits and Systems II: Express Briefs, vol. 66, no. 12, pp. 2022-2026, Dec. 2019.
8) M. Rezvanyvardom and A. Mirzaei, "Zero-Voltage Transition Nonisolated Bidirectional Buck–Boost DC–DC Converter With Coupled Inductors," in IEEE Journal of Emerging and Selected Topics in Power Electronics, vol. 9, no. 3, pp. 3266-3275, June 2021.
9) B. Chandrasekar et al., "Non-Isolated High-Gain Triple Port DC–DC Buck-Boost Converter With Positive Output Voltage for Photovoltaic Applications," in IEEE Access, vol. 8, pp. 113649-113666, 2020.
10) L. Callegaro, M. Ciobotaru, D. J. Pagano, E. Turano and J. E. Fletcher, "A Simple Smooth Transition Technique for the Noninverting Buck–Boost Converter," in IEEE Transactions on Power Electronics, vol. 33, no. 6, pp. 4906-4915, June 2018.
11) F. Méndez-Díaz, B. Pico, E. Vidal-Idiarte, J. Calvente and R. Giral, "HM/PWM Seamless Control of a Bidirectional Buck–Boost Converter for a Photovoltaic Application," in IEEE Transactions on Power Electronics, vol. 34, no. 3, pp. 2887-2899, March 2019.

iJETRM
International Journal of Engineering Technology Research & Management
(IJETRM)
https://ijetrm.com/

12) M. R. Banaei and S. G. Sani, "Analysis and Implementation of a New SEPIC-Based Single-Switch Buck–Boost DC–DC Converter With Continuous Input Current," in IEEE Transactions on Power Electronics, vol. 33, no. 12, pp. 10317-10325, Dec. 2018.
13) R. Pandey and B. Singh, "A Power-Factor-Corrected LLC Resonant Converter for Electric Vehicle Charger Using Cuk Converter," in IEEE Transactions on Industry Applications, vol. 55, no. 6, pp. 6278-6286, Nov.-Dec. 2019.
14) B. R. Ananthapadmanabha, R. Maurya and S. R. Arya, "Improved Power Quality Switched Inductor Cuk Converter for Battery Charging Applications," in IEEE Transactions on Power Electronics, vol. 33, no. 11, pp. 9412-9423, Nov. 2018.
15) H. Ardi and A. Ajami, "Study on a High Voltage Gain SEPIC-Based DC–DC Converter With Continuous Input Current for Sustainable Energy Applications," in IEEE Transactions on Power Electronics, vol. 33, no. 12, pp. 10403-10409, Dec. 2018.
16) S. Kakkar et al., "Design and Control of Grid-Connected PWM Rectifiers by Optimizing Fractional Order PI Controller Using Water Cycle Algorithm," in IEEE Access, vol. 9, pp. 125941-125954, 2021.
17) M. Ali, H. Kotb, K. M. Aboras and N. H. Abbasy, "Design of Cascaded PI-Fractional Order PID Controller for Improving the Frequency Response of Hybrid Microgrid System Using Gorilla Troops Optimizer," in IEEE Access, vol. 9, pp. 150715-150732, 2021.
18) M. Jafari, Z. Malekjamshidi and M. R. Islam, "Optimal Design of a Multiwinding High-Frequency Transformer Using Reluctance Network Modeling and Particle Swarm Optimization Techniques for the Application of PV-Linked Grid-Connected Modular Multilevel Inverters," in IEEE Journal of Emerging and Selected Topics in Power Electronics, vol. 9, no. 4, pp. 5083-5096, Aug. 2021.
19) S. Figueiredo and R. Nayana Alencar Leão e Silva Aquino, "Hybrid MPPT Technique PSO-P&O Applied to Photovoltaic Systems Under Uniform and Partial Shading Conditions," in IEEE Latin America Transactions, vol. 19, no. 10, pp. 1610-1617, Oct. 2021.
20) C. Tao, X. Wang, F. Gao and M. Wang, "Fault diagnosis of photovoltaic array based on deep belief network optimized by genetic algorithm," in Chinese Journal of Electrical Engineering, vol. 6, no. 3, pp. 106-114, Sept. 2020.
21) D. A. Nugraha, K. L. Lian and Suwarno, "A Novel MPPT Method Based on Cuckoo Search Algorithm and Golden Section Search Algorithm for Partially Shaded PV System," in Canadian Journal of Electrical and Computer Engineering, vol. 42, no. 3, pp. 173-182, Summer 2019.
22) M. Dehghani, M. Taghipour, G. B. Gharehpetian and M. Abedi, "Optimized Fuzzy Controller for MPPT of Grid-connected PV Systems in Rapidly Changing Atmospheric Conditions," in Journal of Modern Power Systems and Clean Energy, vol. 9, no. 2, pp. 376-383, March 2021.
23) Y. -P. Huang, M. -Y. Huang and C. -E. Ye, "A Fusion Firefly Algorithm With Simplified Propagation for Photovoltaic MPPT Under Partial Shading Conditions," in IEEE Transactions on Sustainable Energy, vol. 11, no. 4, pp. 2641-2652, Oct. 2020.
24) S. Motahhir et al., "Optimal Energy Harvesting From a Multistrings PV Generator Based on Artificial Bee Colony Algorithm," in IEEE Systems Journal, vol. 15, no. 3, pp. 4137-4144, Sept. 2021.
25) F. A. Alturki, H. O. Omotoso, A. A. Al-Shamma'a, H. M. H. Farh and K. Alsharabi, "Novel Manta Rays Foraging Optimization Algorithm Based Optimal Control for Grid-Connected PV Energy System," in IEEE Access, vol. 8, pp. 187276-187290, 2020.
26) A. K. Singh, A. K. Mishra, K. K. Gupta, P. Bhatnagar and T. Kim, "An Integrated Converter With Reduced Components for Electric Vehicles Utilizing Solar and Grid Power Sources," in IEEE Transactions on Transportation Electrification, vol. 6, no. 2, pp. 439-452, June 2020.
27) J. C. d. S. de Morais, J. L. d. S. de Morais and R. Gules, "Photovoltaic AC Module Based on a Cuk Converter With a Switched-Inductor Structure," in IEEE Transactions on Industrial Electronics, vol. 66, no. 5, pp. 3881-3890, May 2019.